

Quenching of Metals Containing Impurity. II. Substitutional Impurity in Body-Centered-Cubic Metals*

M. DOYAMA

Argonne National Laboratory, Argonne, Illinois

(Received 20 February 1967)

Impurity-vacancy complexes and two-vacancy-impurity-atom complexes up to the next-nearest-neighbor interaction are shown and classified. The kinetic equations between vacancies and impurity atoms in body-centered cubic crystals for the nearest-neighbor interaction alone and for the nearest- and next-nearest-neighbor interactions are presented. Applications of these equations to the thermal equilibrium and to the reaction during quenching and aging are treated. The critical temperatures or freezing temperatures which determine the status after the quench are given. The cooling rate near the critical temperature determines the quenched status. The analytical treatment is in good agreement with the results of the actual change during quenching calculated by a digital computer.

I. INTRODUCTION

THE motion of impurity atoms in a quenched metal is often much faster than that in an annealed metal.¹ This is due to the quenched-in excess vacancies, which stay in the quenched metal and accelerate the motion of impurity atoms. The vacancies present at a high temperature associate with impurity atoms during quenching and also during annealing. It has been shown that the point defects in pure metals and dilute alloys play an important role in quenching, equilibrium, and diffusion experiments. Two major factors for the interaction between vacancies and impurity atoms and between impurity atoms themselves are the distortion of lattice around the impurity atoms² and the electrostatic interaction between vacancies and impurity atoms.³

Hasiguti^{4,5} has found an empirical rule on the vacancy-impurity binding energy in aluminum. He related the binding energy, the valence, and the atomic diameter of a solute impurity atom. Doyama^{6,7} related the vacancy-impurity binding energy in aluminum and the solubility limit of the impurity in aluminum. He also found that the heat of solution of impurity in aluminum is about twice that of the binding energy. Doyama and Cotterill⁸ refined this relation.

The total fractional concentration of vacancies in a body-centered cubic metal containing impurity at a thermal equilibrium is given by

$$C = C_1 + C_{vi} \\ = A_1(1 - 9C_{ii}) \exp(-E_v^F/kT) \\ + 8C_{ii}A_2 \exp\{-(E_v^F - B_{vi})/kT\}, \quad (1)$$

* Based on work performed under the auspices of the U. S. Atomic Energy Commission.

¹ For example, D. Turnbull, in *Solid State Physics*, edited by F. Seitz and D. Turnbull (Academic Press Inc., New York, 1956), Vol. 3, p. 225.

² For example, R. Swalin, *Acta Met.* **5**, 443 (1957).

³ For example, D. Lazarus, *Phys. Rev.* **93**, 973 (1954).

⁴ R. R. Hasiguti, *J. Phys. Soc. Japan* **20**, 625 (1965).

⁵ R. R. Hasiguti, *J. Phys. Soc. Japan* **21**, 1223 (1966).

⁶ M. Doyama, *Phys. Rev.* **148**, 681 (1966).

⁷ M. Doyama, *Phys. Letters* **21**, 395 (1966).

⁸ M. Doyama and R. M. J. Cotterill, *Phys. Letters* **23**, 58 (1966).

where C_{ii} is the fractional concentration of impurity atoms. The first term represents the fractional concentration of free vacancies C_1 , and the second term represents the fractional concentration of impurity atom-vacancy complexes C_{vi} . A_1 and A_2 are constants, and E_v^F is the energy required to form a vacancy far from an impurity atom. B_{vi} is the binding energy between a vacancy and an impurity atom. Only the substitutional impurity is considered here.

Vacancies present at a high temperature can be frozen in by rapid cooling. In a practical quench, however, the quench speed is finite; and because of this, the reaction between vacancies and other defects progress even during a high-speed quench. The quenched status, therefore, is not the same as that of quenching temperature. Koehler, Seitz, and Bauerle⁹ first investigated this problem. They realized that there exists a critical temperature T^* , above which the reaction is fast enough to maintain a thermal equilibrium, and below which the reaction is too slow to maintain the thermal equilibrium between vacancies and divacancies. Kimura, Maddin, and Kuhlmann-Wilsdorf¹⁰ also discussed this problem. Koehler, de Jong, and Seitz^{11,12} extended this treatment. Fujiwara¹³ analyzed the formation of divacancies during quenching by means of a digital computer.

Cotterill¹⁴ also analyzed the reaction between vacancies and impurity atoms by use of an analog computer. Mori,¹⁵ Meshii and Kauffman^{15,16} experimentally

⁹ J. S. Koehler, F. Seitz, and J. E. Bauerle, *Phys. Rev.* **107** 1499 (1957).

¹⁰ H. Kimura, R. Maddin, and D. Kuhlmann-Wilsdorf, *Acta Met.* **7**, 145 (1959); **7**, 154 (1959).

¹¹ M. de Jong and J. S. Koehler, *Phys. Rev.* **129**, 40 (1963); **129**, 49 (1963).

¹² J. S. Koehler, M. de Jong, and F. Seitz, *J. Phys. Soc. Japan* **18**, Suppl. III, 1 (1963).

¹³ H. Fujiwara, Technical Report, University of Illinois, 1960 (unpublished).

¹⁴ R. M. J. Cotterill, in *Lattice Defects in Quenched Metals*, edited by R. M. J. Cotterill, M. Doyama, J. J. Jackson, and M. Meshii (Academic Press Inc., New York, 1965), p. 97.

¹⁵ T. Mori, M. Meshii, and J. W. Kauffman, *J. Appl. Phys.* **33**, 2776 (1962).

¹⁶ J. W. Kauffman and M. Meshii, in *Lattice Defects in Quenched Metals*, edited by R. M. J. Cotterill, M. Doyama, J. J. Jackson, and M. Meshii (Academic Press Inc., New York, 1965), p. 77.

studied the process that occurred during quenching. This treatment was extended by Flynn, Bass, and Lazarus.^{17,18} In the previous paper⁶ the reactions between vacancies and impurity during quenching and annealing were discussed for face-centered cubic metals. In this paper the same treatment is extended to the interaction between substitutional impurity atoms and vacancies in body-centered cubic metals.

II. VACANCY-IMPURITY COMPLEXES

When vacancies associate with impurity atoms, many configurations of vacancy-impurity clusters are formed. The simplest of these is the vacancy and impurity complexes whose positions are nearest neighbor [shown in Fig. 1(a)]. This configuration will hereafter be called type-I impurity-vacancy complex. Since the next nearest neighbor is only $2/\sqrt{3}$ times the nearest-neighbor distance and the next-next-nearest neighbor is $2\sqrt{2}/\sqrt{3}$ times the nearest-neighbor distance in a body-centered cubic metal, the interactions up to next-nearest neighbor are considered in this paper. The next-nearest-neighbor vacancy-impurity complex is shown in Fig. 1(b). This configuration will be called a type-II impurity-vacancy complex.

The configurations of two vacancy-impurity complexes are shown in Figs. 2 and 3. In Fig. 2(a)–2(f), an impurity atom has two vacancies in the nearest-neighbor positions or in the next-nearest-neighbor positions. These are called here $71^\circ V-i-V$, $109^\circ V-i-V$, $180^\circ(\text{I}) V-i-V$, $90^\circ V=i=V$, $144^\circ V-i=V$, and $180^\circ(\text{II}) V=i=V$. One bar represents the nearest-neighbor bond, and a double bar represents the next-nearest-neighbor bond. When an impurity atom is attached to a divacancy (nearest-neighbor type-I or next-nearest-neighbor type-II), an impurity-divacancy complex is formed. In Fig. 3 the configurations of impurity-divacancy complexes are shown. These are $71^\circ i-V-V$, $109^\circ i-V-V$, $180^\circ(\text{I}) i-V-V$, $90^\circ i=V=V$, $144^\circ i-V=V$, $144^\circ i=V-V$, and $180^\circ(\text{II}) i-V=V$. In Figs. 2 and 3 the nearest-neighbor bonds are shown in thick solid

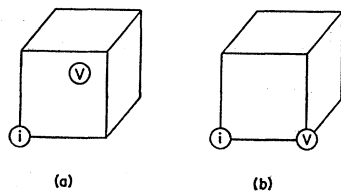


FIG. 1. Impurity-vacancy complexes: (a) Type I, a vacancy and an impurity atom are nearest-neighbor positions to each other; (b) Type II, a vacancy and an impurity atom are next-nearest-neighbor positions to each other.

¹⁷ C. P. Flynn, J. Bass, and D. Lazarus, in *Lattice Defects in Quenched Metals*, edited by R. M. J. Cotterill, M. Doyama, J. J. Jackson, and M. Meshii (Academic Press Inc., New York, 1965), p. 639.

¹⁸ C. P. Flynn, J. Bass, and D. Lazarus, *Phil. Mag.* 11, 521 (1965).

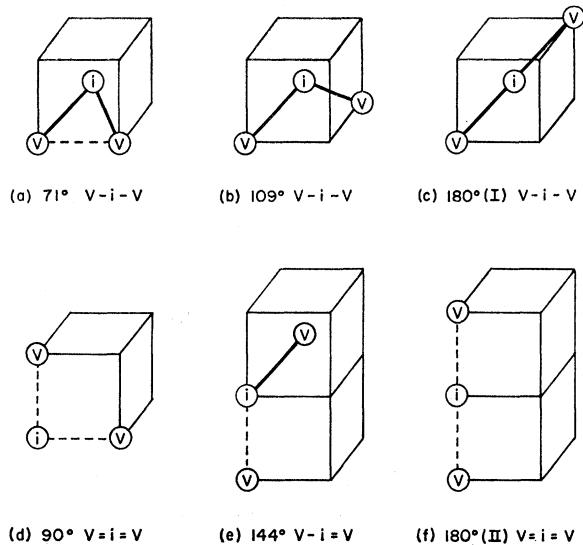


FIG. 2. Impurity two-vacancy complexes. An impurity atom has two vacancies in the nearest-neighbor positions or in the next-nearest-neighbor positions.

lines and the next-nearest-neighbor bonds are shown in broken lines.

III. NEAREST-NEIGHBOR INTERACTION

In this section only the nearest-neighbor interaction is considered; the interaction beyond the next-nearest-neighbor interactions is neglected. The possible configuration of an impurity-vacancy complex is only type I [Fig. 1(a)] for this interaction.

A. Kinetic Equations

The kinetic equations between vacancies and substitutional impurity atoms in body-centered cubic metals are

$$\frac{dC_1}{dt} = -56\nu_1 C_1 C_i \exp\left(-\frac{E_v^M}{kT}\right) + 7\nu_1 C_{vi} \exp\left(-\frac{E_v^M + B_{vi}}{kT}\right), \quad (2)$$

$$\frac{dC_{vi}}{dt} = -\frac{dC_1}{dt}, \quad (3)$$

where C_1 and C_{vi} are the fractional concentrations of single vacancies and impurity-vacancy complexes; ν_1 is the frequency coefficient for the migration of a vacancy. E_v^M is the activation energy for the migration of a vacancy and B_{vi} is the binding energy between a vacancy and an impurity atom. Here the annealing of vacancies to sinks is neglected.

The geometrical factors in Eq. (2) were calculated as follows. A substitutional impurity atom has eight

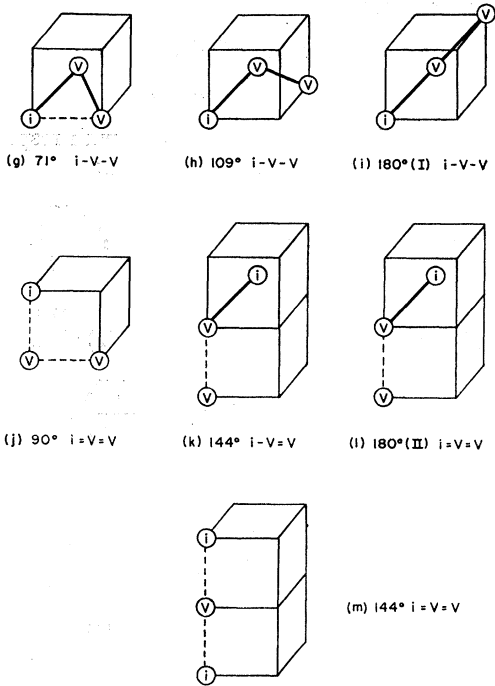


FIG. 3. Impurity divacancy complexes. A divacancy has an impurity atom in the nearest-neighbor position or the next-nearest-neighbor position.

nearest neighbors, each of which has seven sites to make a vacancy-impurity complex. The total number to make an impurity-vacancy complex is 56. An impurity-vacancy complex has seven sites to break up into a vacancy and an isolated impurity; the coefficient of the second term in Eq. (2) is 7.

B. Thermal Equilibrium

At a thermal equilibrium the formation of impurity-vacancy complexes and the breakup of complexes are equal. The fractional concentration of impurity-vacancy complexes C_{vi} is given by

$$C_{vi} = 8C_i C_1 \exp(B_{vi}/kT). \tag{4}$$

When the total fractional concentration C_t , which is the sum of the fractional concentration of free vacancies C_1 and that of associated vacancies C_{vi} , and the total impurity concentration C_{it} are given, i.e.,

$$C_t = C_1 + C_{vi}, \tag{5}$$

$$C_{it} = C_{vi} + C_i, \tag{6}$$

then the fractional concentration of impurity-vacancy complexes C_{vi} and the fractional concentration of free vacancies C_1 can be expressed in terms of known quantities.

$$C_{vi} = \frac{1}{16} (8(C_t + C_{it}) + \exp(-B_{vi}/kT) - [\{8(C_t + C_{it}) + \exp(-B_{vi}/kT)\}^2 - 256C_{it}C_t]^{1/2}), \tag{7}$$

$$C_1 = C_t - C_{vi} = -\frac{1}{16} (8(C_{it} - C_t) + \exp(-B_{vi}/kT) - [\{8(C_t + C_{it}) + \exp(-B_{vi}/kT)\}^2 - 256C_{it}C_t]^{1/2}), \tag{8}$$

where B_{vi} is the binding energy between a vacancy and an impurity atom. The equilibrium fractional concentration of free single vacancies C_1 and the fractional concentration of impurity-vacancy complexes C_{vi} are plotted with a function of temperature (Figs. 4, 5, and 6). Figure 4 is for $C_t = 10^{-6}$ and $C_{it} = 10^{-3}$. Figure 5 is for $C_t = 10^{-5}$ and $C_{it} = 10^{-3}$. Figure 6 is for $C_t = 10^{-5}$ and $C_{it} = 10^{-4}$. As can be seen from these figures, the logarithm of C_{vi} against $1/T$ gives straight lines for low binding energy or for high temperature. For this case most of the defects are single vacancies. Therefore in Eq. (4) C_1 can be replaced by C_t and C_i can be replaced by C_{it} ; both are constants for a given alloy and given total concentration of voids. In this region

$$C_{vi} \cong 8C_{it}C_t \exp(B_{vi}/kT). \tag{9}$$

The tangent of C_{vi} curve is proportional to the impurity-vacancy binding energy B_{vi} . Figures 4, 5, and 6 also show that the plot of C_1 is a straight line for high binding energy and low temperature. Under these conditions in Eq. (4), C_{vi} can be replaced by C_t and C_i can be replaced by $C_{it} - C_t$; both of these values are constant for a given alloy and given total concentration of voids. Equation (4) becomes

$$C_1 \cong \frac{1}{8} \frac{C_t}{C_{it} - C_t} \exp\left(-\frac{B_{vi}}{kT}\right). \tag{10}$$

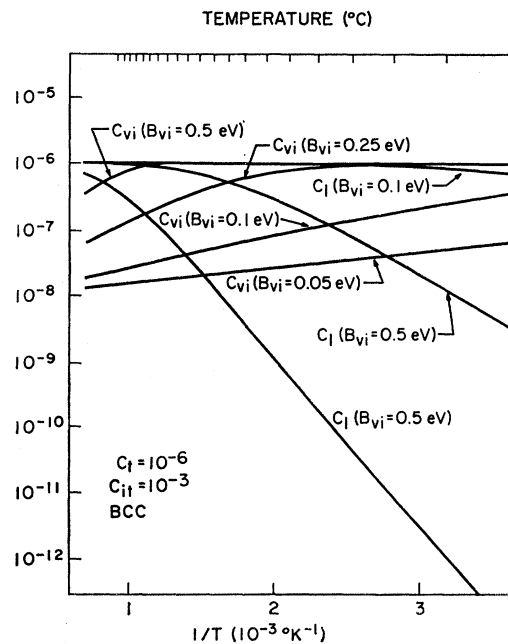


FIG. 4. Equilibrium fractional concentration of free vacancies C_1 and impurity-vacancy complexes C_{vi} versus temperature. The total fractional concentration of impurity atoms C_{it} is 10^{-3} , and the total fractional concentration of voids is 10^{-6} .

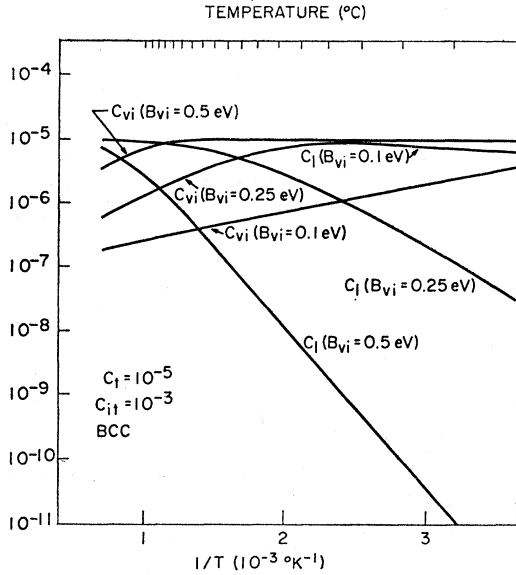


FIG. 5. Equilibrium fractional concentrations of free vacancies C_1 and impurity-vacancy complexes C_{vi} versus temperature. The total fractional concentration of impurity atoms C_{ii} is 10^{-3} , and the total fractional concentration of voids is 10^{-6} .

The slope of the C_1 curve is again proportional to B_{vi} . The slope is $-B_{vi}/2.303k$, where k is Boltzmann's constant.

C. Formation of Impurity-Vacancy Complexes during Quenching

Before a specimen is quenched, free vacancies and impurity-vacancy complexes are in thermal equilibrium at a temperature T_0 , and the temperature of the specimen drops very rapidly during quenching. Impurity-vacancy complexes are formed even during a rapid quench. As has been discussed for face-centered cubic metals,⁶ there exists a critical temperature T^* above which the reaction between single vacancies and vacancy-impurity complexes is still in thermal equilibrium. Below T^* the single vacancies do not move fast enough to maintain the thermal equilibrium. It is assumed here that no vacancies anneal to sinks during quenching. This assumption is not very serious because the annealing of vacancies above T^* does not alter the discussion, and only lowers the quenching temperature. The annealing of vacancies below T^* is negligible; this is the definition of T^* . The kinetic equation is

$$\frac{dC_1}{dt} = -56\nu_1 C_1 C_i \exp\left(-\frac{E_v^M}{kT}\right) + 7\nu_1 C_{vi} \exp\left(-\frac{E_v^M + B_{vi}}{kT}\right). \quad (2)$$

Since it is assumed that no vacancies anneal to sinks

during quenching,

$$C_i = \text{const} = C_1 + C_{vi}, \quad (11)$$

$$C_{it} = \text{const} = C_{vi} + C_i. \quad (12)$$

Differentiating Eqs. (4), (11), and (12) with respect to time t , the following equation is obtained:

$$\frac{dT}{dt} = \frac{kT^2}{8B_{vi}C_1C_i} \left\{ \exp\left(-\frac{B_{vi}}{kT}\right) + 8(C_i + C_1) \right\} \frac{dC_1}{dt}. \quad (13)$$

The rate of the formation of single vacancies at equilibrium is given by the first term of Eq. (2); i.e.,

$$\left(\frac{dC_1}{dt}\right)_e = -56\nu_1 C_1 C_i \exp\left(-\frac{E_v^M}{kT}\right). \quad (14)$$

Equation (13) can be rewritten as

$$\left(\frac{dT}{dt}\right)_{T=T^*} = - \left[\frac{7\nu_1 kT^2}{B_{vi}} \exp\left(-\frac{E_v^M}{kT}\right) \times \left\{ 8(C_i + C_1) + \exp\left(-\frac{B_{vi}}{kT}\right) \right\} \right]_{T=T^*}, \quad (15)$$

where

$$C_1 = -\frac{1}{16} \left\{ 8(C_{ii} - C_i) + \exp(-B_{vi}/kT^*) - \left[\{ 8(C_i + C_{ii}) + \exp(-B_{vi}/kT^*) \}^2 - 256C_{ii}C_i \right]^{1/2} \right\},$$

and

$$C_i = -\frac{1}{16} \left\{ 8(C_i - C_{ii}) + \exp(-B_{vi}/kT^*) - \left[\{ 8(C_i + C_{ii}) + \exp(-B_{vi}/kT^*) \}^2 - 256C_{ii}C_i \right]^{1/2} \right\}.$$

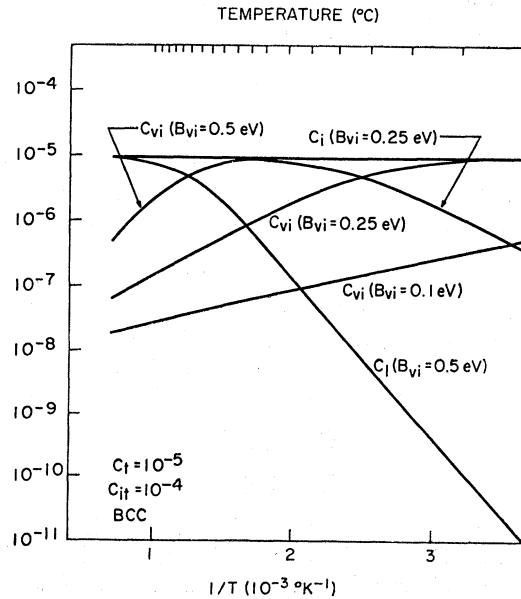


FIG. 6. Equilibrium fractional concentrations of free vacancies C_1 and impurity-vacancy complexes C_{vi} versus temperature. The total fractional concentration of impurity atoms C_{ii} is 10^{-4} , and the total fractional concentration of voids is 10^{-6} .

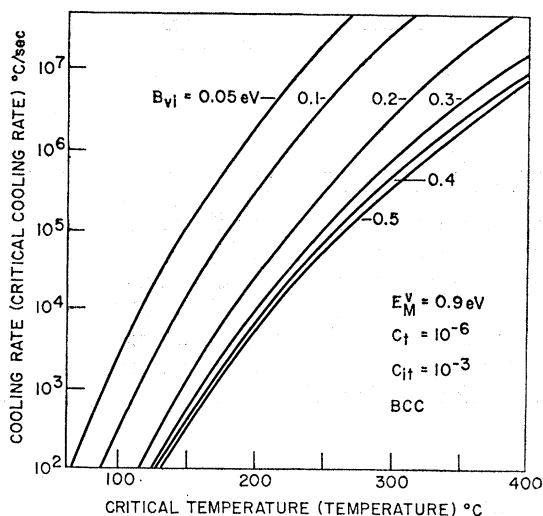


FIG. 7. The values of critical cooling rate versus temperature. The activation energy for the motion of a vacancy is 0.9 eV. The fractional concentrations of total voids C_t and total impurity atoms C_{it} are 10^{-6} and 10^{-3} , respectively. The binding energies B_{vi} of an impurity-vacancy complex are shown in the figure. This can be also directly used for cooling-rate-versus-critical-temperature relations.

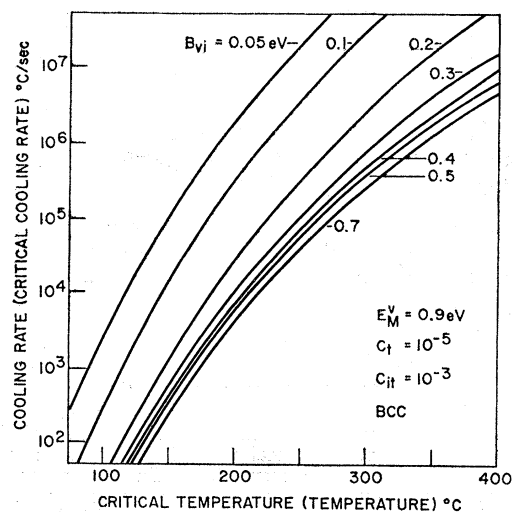


FIG. 9. The values of critical cooling rate versus temperature. The activation energy for the motion of a vacancy is 0.9 eV. The fractional concentrations of total voids C_t and total impurity atoms C_{it} are 10^{-5} and 10^{-3} , respectively. The binding energies B_{vi} of an impurity-vacancy complex are shown in the figure. This can be directly used for cooling-rate-versus-critical-temperature relations.

The right side of Eq. (15) is called the critical cooling rate. The values of the critical cooling rate are plotted in Figs. 7-10 for the case $E_M^V = 0.9$ eV; ν_1 is taken to be 10^{13} sec $^{-1}$. The activation energy for the self-diffusion in tungsten is reported to be 5.23 eV.¹⁹ Schultz²⁰ found the

formation energy of a vacancy in tungsten to be 3.30 eV. If the self-diffusion is conducted by a vacancy mechanism, the activation energy for the migration of a vacancy is 1.93 eV,²⁰ which is 37% of the formation energy of a vacancy. If this ratio is about the same in α iron, then the activation energy for the motion of a single vacancy in α iron is about 0.9 eV. The activation

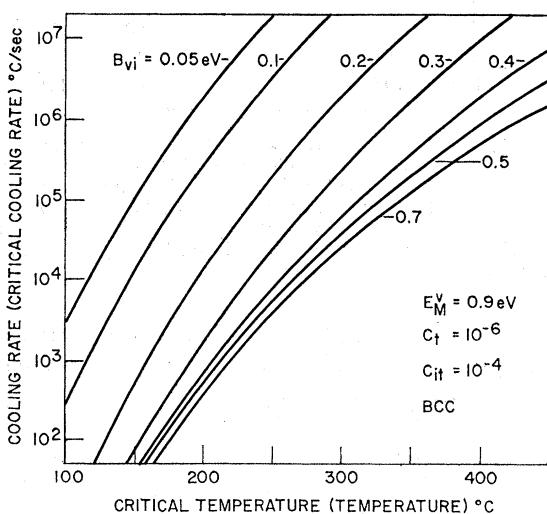


FIG. 8. The values of critical cooling rate versus temperature. The activation energy for the motion of a vacancy is 0.9 eV. The fractional concentrations of total voids C_t and total impurity atoms C_{it} are 10^{-6} and 10^{-4} , respectively. The binding energies B_{vi} of an impurity-vacancy complex are shown in the figure. This can be also directly used for cooling-rate-versus-critical-temperature relations.

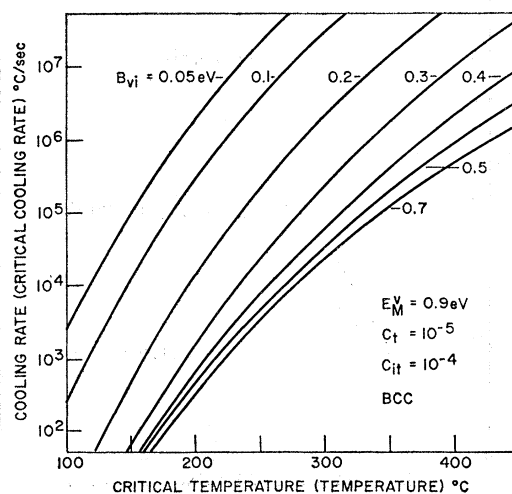


FIG. 10. The values of critical cooling rate versus temperature. The activation energy for the motion of a vacancy is 0.9 eV. The fractional concentrations of total voids C_t and total impurity atoms C_{it} are 10^{-5} and 10^{-4} , respectively. The binding energies B_{vi} of an impurity-vacancy complex are shown in the figure. This can be directly used for cooling-rate-versus-critical-temperature relations.

¹⁹ W. Darneberg, *Metallurgia* **15**, 977 (1961).

²⁰ H. Schultz, in *Lattice Defects in Quenched Metals*, edited by R. M. J. Cotterill, M. Doyama, J. J. Jackson, and M. Meshii (Academic Press Inc., New York, 1965), p. 761.

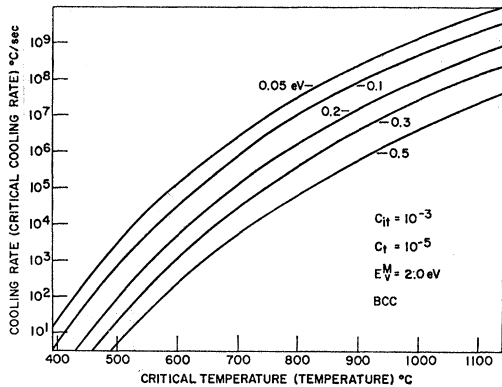


FIG. 11. The values of critical cooling rate versus temperature. The activation energy for the motion of a vacancy is 2.0 eV. The fractional concentrations of total voids C_t and total impurity atoms C_{it} are 10^{-3} and 10^{-5} , respectively. The binding energies B_{vi} of an impurity-vacancy complex are shown in the figure. This can be directly used for cooling-rate-versus-critical-temperature relations.

energy for self-diffusion is reported to be 2.60 eV.²¹ Therefore, Figs. 7–10 are probably close to the case for α iron. Figure 11 is for the case $E_v^M = 2.0$ eV, which is close to the case for tungsten. The values of the total fractional concentration of impurity atoms C_{it} and the total concentration of voids are shown in these figures. Knowing the cooling rate during the quench, one can find the critical temperature T^* using these figures. If one plots the cooling rate during quenching on Figs. 7–10, then where the cooling curve is above the critical-cooling-rate curve, the reaction between vacancies and impurity atoms is in thermal equilibrium. Where the cooling curve falls below the critical-cooling-

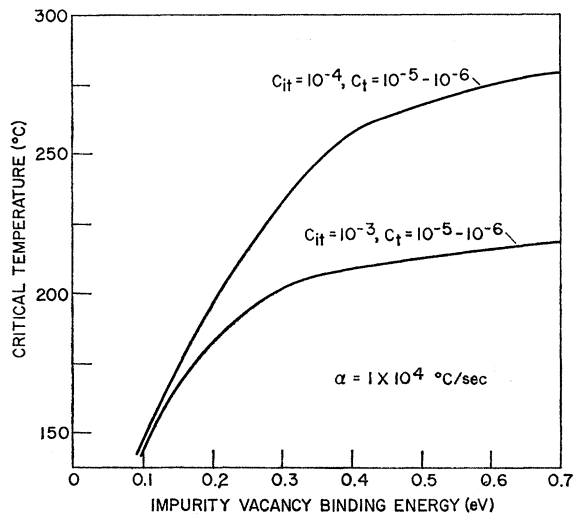


FIG. 12. Relation between critical temperature and the binding energy between a vacancy and an impurity atom as a function of the fractional concentration of total vacancies and of impurity. The cooling rate is taken to be 1×10^4 deg/sec.

²¹ F. S. Buffington, I. D. Bakalar, and M. Cohen, *Physics of Powder Metallurgy* (McGraw-Hill Book Company, Inc., New York, 1951), Chap. 6; J. Met. 4, 859 (1952).

rate curve, the reaction is frozen. The intersection of the cooling curve and the critical-cooling-rate curve gives the critical temperature T^* . The critical temperature depends upon the cooling rate only at the critical temperature, on the binding energy between an impurity atom and a vacancy, and on the activation energy for the migration of a vacancy. The shape of a quench curve is not important if the cooling rate at T^* stays the same. The critical temperature becomes lower as the binding energy of a vacancy and an impurity atom becomes lower (see Fig. 12). The critical temperature is insensitive to the total concentration of voids. The critical temperature is also insensitive to the concentration of impurity if the impurity-vacancy

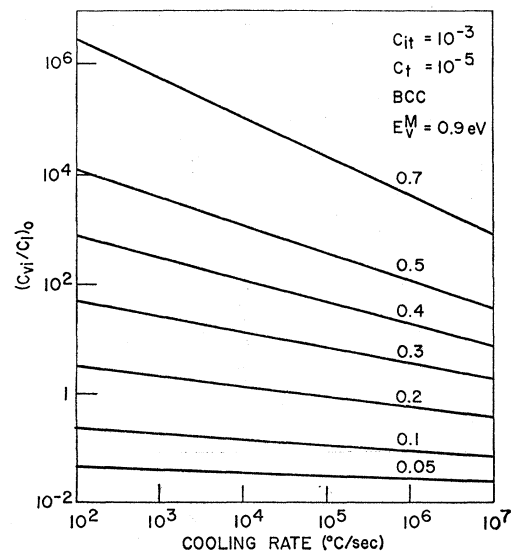


FIG. 13. The logarithm of the ratio of the fractional concentration of impurity-vacancy complexes to that of free vacancies after quenching versus the logarithm of cooling rate. The activation energy for the motion of a vacancy is taken to be 0.9 eV. The fractional concentrations of total voids C_t and total impurity atoms C_{it} are 10^{-3} and 10^{-5} , respectively. The figure shows a straight line.

binding energy is low. The fractional concentration of impurity-vacancy complexes after the quench is given by

$$(C_{vi})_0 = 8(C_1)_0(C_i)_0 \exp(B_{vi}/kT^*)$$

or

$$\left(\frac{C_{vi}}{C_1}\right)_0 = 8(C_i)_0 \exp\left(\frac{B_{vi}}{kT^*}\right). \quad (16)$$

This ratio is plotted in Fig. 13 as a function of the cooling rate. The plot of the logarithm of $(C_{vi}/C_1)_0$ versus the logarithm of the cooling rate gives a straight line (Fig. 13). This can be shown as follows. Equation (15) can be written as

$$-\left(\frac{dT}{dt}\right)_{T=T^*} = \frac{56\nu_1 C_i k T^{*2}}{B_{vi}} \exp\left(-\frac{E_v^M}{kT^*}\right), \quad (17)$$

when $8C_i \gg \exp(-B_{vi}/kT^*)$. T^* is near 250°C for the case of iron; this condition is satisfied when $B_{vi} > 0.23$ eV. Taking the logarithm of Eq. (16) and Eq. (17), one obtains the following relation:

$$\ln\left(\frac{C_{vi}}{C_1}\right)_0 = -\frac{B_{vi}}{E_v^M} \ln\left(-\frac{dT}{dt}\right)_{T=T^*} + \ln 8C_i + \frac{B_{vi}}{E_v^M} \ln \frac{56\nu_1 C_i k T^{*2}}{B_{vi}}. \quad (18)$$

The plot of the logarithm of the quench speed against $\ln(C_{vi}/C_1)_0$ shows a straight line because the last term is not very sensitive to (dT/dt) . The slope of the line is $-B_{vi}/E_v^M$. When $8C_i \ll \exp(-B_{vi}/kT^*)$, i.e., for the

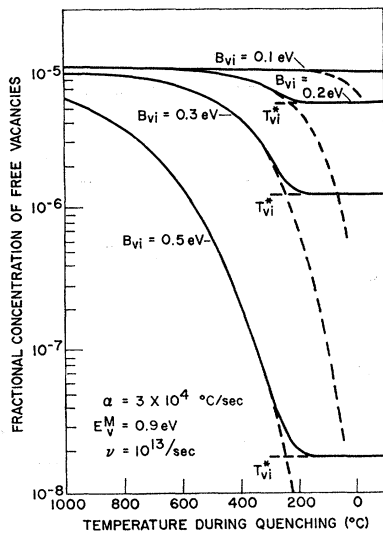


FIG. 14. The change of free vacancy concentration during quenching. The activation energy for the motion of a vacancy is taken to be 0.9 eV. The frequency factor is 10^{13} sec^{-1} . The cooling rate is $3 \times 10^4 \text{ deg/sec}$. Dashed lines are for equilibrium. T_{vi}^* is the critical temperature.

case of iron, $B_{vi} < 0.23$ eV,

$$\left(\frac{dT}{dt}\right)_{T=T^*} \cong \frac{7\nu_1 k T^{*2}}{B_{vi}} \exp\left(-\frac{E_v^M + B_{vi}}{kT^*}\right), \quad (19)$$

$$\ln\left(\frac{C_{vi}}{C_1}\right)_0 = -\frac{B_{vi}}{E_v^M + B_{vi}} \ln\left(\frac{dT}{dt}\right)_{T=T^*} + \ln C_i + \frac{B_{vi}}{E_v^M + B_{vi}} \ln \frac{7\nu_1 k T^{*2}}{B_{vi}}. \quad (20)$$

The curve is again a straight line and the slope is $-B_{vi}/(E_v^M + B_{vi})$.

The kinetic equations [(2) and (3)] were numerically integrated by means of a CDC 3600 digital computer. The activation energy for the migration of a vacancy

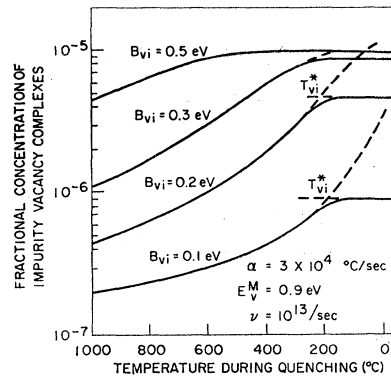


FIG. 15. The change of the fractional concentration of impurity-vacancy complexes during quenching. The activation energy for the motion of a vacancy is taken to be 0.9 eV. The frequency factor is 10^{13} sec^{-1} . The cooling rate is $3 \times 10^4 \text{ deg/sec}$. Dashed lines are for equilibrium. T_{vi}^* is the critical temperature.

E_v^M , the cooling rate α , and the vibrational frequency ν were taken to be 0.9 eV, $3 \times 10^4 \text{ C/sec}$, and 10^{13} sec^{-1} , respectively. The values of the binding energy of impurity-vacancy complexes are taken to be 0.1, 0.2, 0.3, and 0.5 eV. The change of the fractional concentration of free vacancies and the change of the fractional concentration of impurity-vacancy complexes during quenching are plotted in Figs. 14 and 15, respectively. The dotted lines are the fractional concentrations at the equilibrium state. The actual concentrations of free vacancies and complexes deviate sharply from the equilibrium curve near the critical temperature. The concentrations of free vacancies or complexes do not change below the critical temperature. The reactions between free vacancies and impurity atoms are frozen. Above the critical temperature the curve coincides with the equilibrium curve. The values of the critical temperature calculated by the integration of kinetic equations are in good agreement with the values found in Fig. 9. The concentrations of free vacancies and impurity-vacancy complexes calculated from Eq. (15) are also in good agreement with those calculated by the integration of Eqs. (2) and (3).

D. Association of Vacancies and Impurity Atoms during Aging

After a specimen is quenched to a lower temperature some of the quenched-in vacancies will migrate, forming impurity-vacancy complexes during aging. Finally, a quasi-equilibrium state will be obtained. It is assumed that no vacancies anneal out to sinks. Damask and Dienes studied this phenomenon using an analog computer.²²

A specimen will contain the fractional concentration of impurity-vacancy complexes given by

$$(C_{vi})_0 = 8(C_1)_0(C_i)_0 \exp(B_{vi}/kT^*),$$

²² A. C. Damask and G. J. Dienes, Phys. Rev. **120**, 99 (1960).

where

$$(C_1)_0 = C_t - (C_{vi})_0 \quad \text{and} \quad (C_i)_0 = C_{it} - (C_{vi})_0. \quad (21)$$

C_t is the total fractional concentration of voids, C_i is the fractional concentration of free impurity atoms, C_{it} is the total fractional concentration of impurity atoms, and C_{vi} is the fractional concentration of impurity-vacancy complexes. Subzero means the concentrations right after a quench. $(C_{vi})_0$ can be expressed with C_t and C_{it} :

$$(C_{vi})_0 = \frac{1}{2} \left\{ C_t + C_{it} + \frac{1}{8} \exp\left(-\frac{B_{vi}}{kT^*}\right) - \left[\left[C_t + C_{it} + \frac{1}{8} \exp\left(-\frac{B_{vi}}{kT^*}\right) \right]^2 - 4C_t C_{it} \right]^{1/2} \right\}. \quad (22)$$

The rate of change of the fractional concentration of vacancy-impurity atom complexes can be derived from Eqs. (2), (3), (5), and (6), viz.,

$$\frac{dC_{vi}}{dt} = 7\nu_1 \exp\left(-\frac{E_v^M}{kT}\right) \left[8C_{vi}^2 - C_{vi} \times \left\{ 8(C_t + C_{it}) + \exp\left(-\frac{B_{vi}}{kT}\right) \right\} + 8C_t C_{it} \right]. \quad (23)$$

This differential equation can be easily integrated.

$$t = t_0 + \frac{1}{7\nu_1\sqrt{D}} \exp\left(\frac{E_v^M}{kT}\right) \times \ln \frac{16C_{vi} - \{8(C_t + C_{it}) + \exp(-B_{vi}/kT)\} - \sqrt{D}}{16C_{vi} - \{8(C_t + C_{it}) + \exp(-B_{vi}/kT)\} + \sqrt{D}}, \quad (24)$$

where

$$D = \left\{ 8(C_t + C_{it}) + \exp\left(-\frac{B_{vi}}{kT}\right) \right\}^2 - 256C_t C_{it},$$

$$t_0 = \frac{1}{7\nu_1\sqrt{D}} \exp\left(\frac{E_v^M}{kT}\right) \times \ln \frac{16(C_{vi})_0 - \{8(C_t + C_{it}) + \exp(-B_{vi}/kT)\} + \sqrt{D}}{16(C_{vi})_0 - \{8(C_t + C_{it}) + \exp(-B_{vi}/kT)\} - \sqrt{D}}.$$

The characteristic time to form the equilibrium concentration of impurity-vacancy complexes τ is given by

$$\tau = \frac{1}{7\nu_1\sqrt{D}} \exp\left(\frac{E_v^M}{kT}\right). \quad (25)$$

The values of τ are plotted in Fig. 16 for the case $C_{it} = 10^{-3}$ and $C_t = 10^{-5}$. As can be seen in Fig. 16, in the low-temperature region the curve is straight and also in the very-high-temperature region the curve is

straight. It is easy to show that τ is proportional to $\exp(E_v^M/kT)$ for low temperatures when $8(C_t + C_{it}) \gg \exp(-B_{vi}/kT)$ and $T \ll B_{vi}/kT$. τ is proportional to $\exp\{(E_v^M + 2B_{vi})/kT\}$ for high temperatures and when $8(C_t + C_{it}) \ll \exp(-B_{vi}/kT)$.

IV. NEXT-NEAREST-NEIGHBOR INTERACTION

As is discussed in Sec. II, the next-nearest-neighbor interaction is important in body centered cubic metals. In this section the interaction up to the next-nearest-neighbor interaction is considered.

A. Kinetic Equations

The kinetic equations between the fractional concentration of free single vacancies and impurity-vacancy complexes type I and type II are

$$\frac{dC_1}{dt} = -56\nu C_1 C_i \exp\left(-\frac{E_v^M}{kT}\right) + 4\nu C_I \exp\left(-\frac{B_I + E_v^M}{kT}\right) + 4\nu C_{II} \exp\left(-\frac{B_{II} + E_v^M}{kT}\right), \quad (26)$$

$$\frac{dC_I}{dt} = -3\nu C_I \exp\left(-\frac{B_I - B_{II} + E_M^{I-II}}{kT}\right) - 4\nu C_I \exp\left(-\frac{B_I + E_v^M}{kT}\right) + 4\nu C_{II} \exp\left(-\frac{E_M^{I-II}}{kT}\right) + 32\nu C_1 C_i \exp\left(-\frac{E_v^M}{kT}\right), \quad (27)$$

$$\frac{dC_{II}}{dt} = 3\nu C_I \exp\left(-\frac{B_I - B_{II} + E_M^{I-II}}{kT}\right) - 4\nu C_{II} \exp\left(-\frac{E_M^{I-II}}{kT}\right) - 4\nu C_{II} \times \exp\left(-\frac{B_{II} + E_v^M}{kT}\right) + 24\nu C_1 C_i \exp\left(-\frac{E_v^M}{kT}\right), \quad (28)$$

where C_1 , C_I , and C_{II} are the fractional concentrations of free single vacancies, type-I impurity-vacancy complexes, and type-II impurity-vacancy complexes, respectively; ν is the frequency coefficient. Here all of the frequency coefficients are taken to be the same. E_v^M is the activation energy for the migration of a single vacancy. E_M^{I-II} is the activation energy for the migration from type-I to type-II impurity-vacancy complex. B_I and B_{II} are the binding energies of type-I and type-II impurity-vacancy complexes, respectively. The geometrical factors are derived as follows. In Eq. (27) the first term is the formation of type II from type I. There are three sites to make type-II complex. The

second term is the breakup of type-II complex into a single vacancy and isolated impurity atom. The third term is the formation of type-I from type-II complex. Three type-II complexes can make a particular configuration of type-I complex. The last term is the formation of type I by an impurity atom and a free vacancy. An impurity atom has eight nearest-neighbor positions, each of which has four possible sites to make type I (8×4). Similarly the first term of Eq. (16) is the formation of type II from type I. The second term is the formation of type I from type II. The third term is the breakup of type-II complexes into free vacancies and free impurity atoms. The fourth term is the formation of type II by the association of free vacancies and free impurity atoms. The schematic diagram for the energy relation is shown in Fig. 17.

B. Thermal Equilibrium

At a thermal equilibrium, the formation of impurity-vacancy complexes and the breakup of impurity-vacancy complexes are equal and balanced. The left side of Eqs. (26), (27), and (28) are all zero. Therefore,

$$C_I = \xi_I C_1 C_i, \tag{29}$$

$$C_{II} = \xi_{II} C_1 C_i, \tag{30}$$

where

$$\xi_I = 8 \exp(B_I/kT), \tag{31}$$

$$\xi_{II} = 6 \exp(B_{II}/kT). \tag{32}$$

Here C_i , C_1 , C_I , and C_{II} are the fractional concentrations of isolated free impurity atoms, free single vacancies, type-I impurity-vacancy complexes, and type-II impurity-vacancy complexes, respectively. When the

$$C_I = \frac{1}{2} \left\{ \left[\left(C_{ii} - C_i + \frac{1}{\xi_I + \xi_{II}} \right)^2 + \frac{4C_i}{\xi_I + \xi_{II}} \right]^{1/2} - \left(C_{ii} - C_i + \frac{1}{\xi_I + \xi_{II}} \right) \right\}, \tag{35}$$

$$C_i = C_{ii} / \left(1 + \frac{\xi_I + \xi_{II}}{2} \left[\left(C_{ii} - C_i + \frac{1}{\xi_I + \xi_{II}} \right)^2 + \frac{4C_i}{\xi_I + \xi_{II}} \right]^{1/2} - \left(C_{ii} - C_i + \frac{1}{\xi_I + \xi_{II}} \right) \right), \tag{36}$$

$$C_I = \xi_I C_1 C_i, \tag{29}$$

$$C_{II} = \xi_{II} C_1 C_i. \tag{30}$$

Figure 18 shows the equilibrium fractional concentrations of type-I and type-II impurity-vacancy complexes and single vacancies under a given fractional concentration of impurity and total voids. The binding energy of type-II impurity-vacancy complex B_{II} is chosen to be half of that of type I in this case. Figure 19 shows the change in equilibrium fractional concentrations of type-I and type-II impurity-vacancy complexes and single vacancies with a function of the binding energy of type-II impurity-vacancy complex, under given concentrations of impurity and total voids and a given binding energy of type-I impurity-vacancy complex. Figure 20 shows the effect of the fractional concentra-

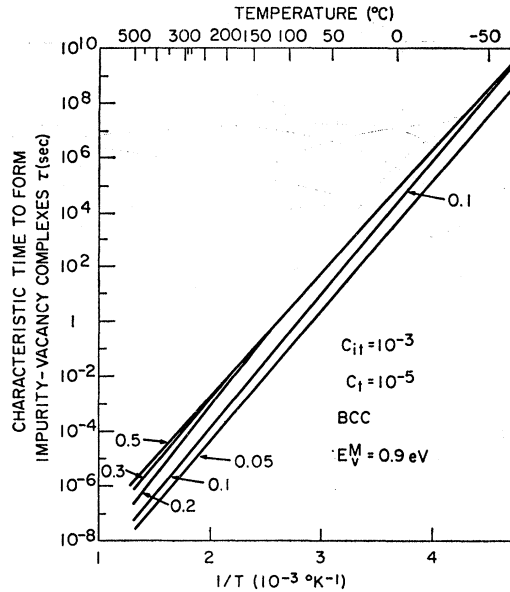


Fig. 16. The characteristic time to form vacancy-impurity complexes versus temperature. The activation energy for the motion of a vacancy is taken to be 0.9 eV. The frequency factor is 10^{18} sec^{-1} . The fractional concentration of total void C_i and total impurity atoms C_{ii} are 10^{-6} and 10^{-3} , respectively.

total fractional concentration of impurity C_{ii} and the total fractional concentration of vacancies (free and associated) C_i are known, the following relations are obtained:

$$C_{ii} = C_i + C_I + C_{II}, \tag{33}$$

$$C_i = C_1 + C_I + C_{II}, \tag{34}$$

tion of impurity on the equilibrium concentration of types-I and -II impurity-vacancy complexes and single vacancies.

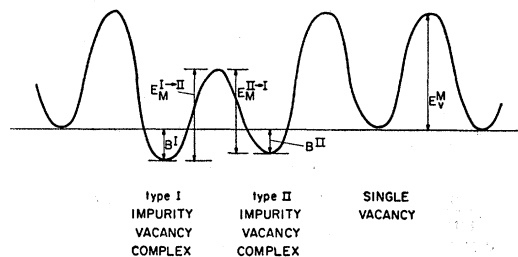


Fig. 17. Schematic energy diagram for impurity-vacancy complexes type-I and type-II and single vacancies, their conversion, and breakup.

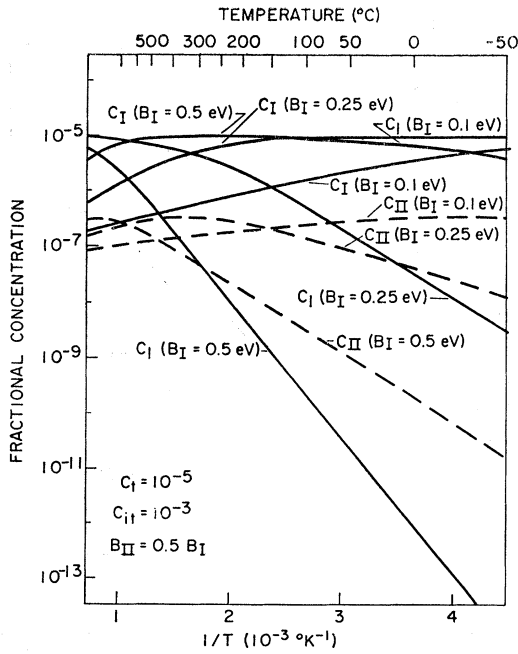


FIG. 18. Equilibrium fractional concentrations of free vacancies C_I and impurity-vacancy complexes, type I (C_I) and type II (C_{II}) versus temperature. The total fractional concentrations of impurity atoms C_{it} and total voids C_t are 10^{-3} and 10^{-5} , respectively. B_{II} is taken to be $0.5 B_I$. The binding energies of type-I impurity-vacancy complex are shown in the figure.

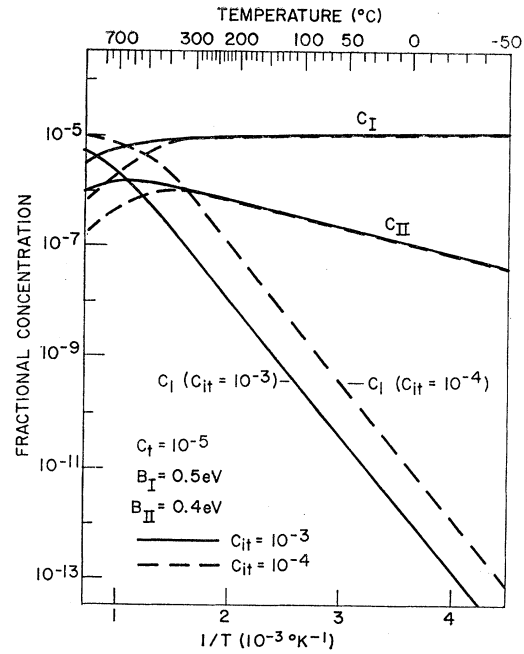


FIG. 20. Equilibrium fractional concentrations of free vacancies C_I and impurity-vacancy complexes, type I (C_I) and type II (C_{II}) versus temperature. The fractional concentrations of total impurity are taken to be 10^{-3} and 10^{-4} and shown in solid lines and dashed lines, respectively. The binding energies of type-I and type-II impurity-vacancy complexes are taken to be 0.5 and 0.4 eV, respectively.

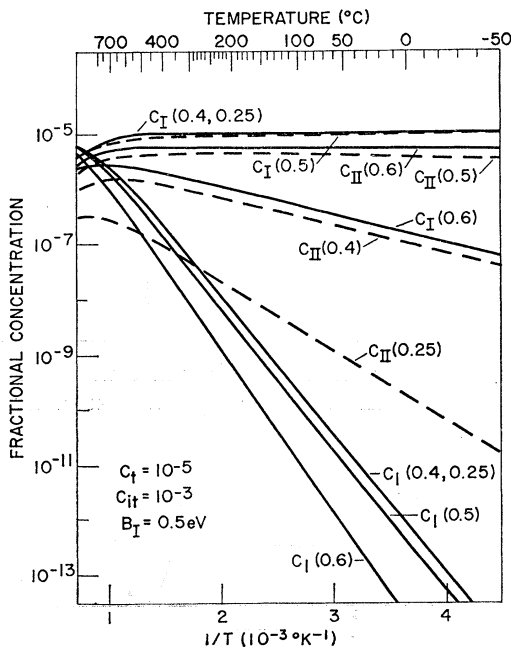


FIG. 19. Equilibrium fractional concentrations of free vacancies C_I and impurity-vacancy complexes, type I (C_I) and type II (C_{II}) versus temperature. The fractional concentrations of total impurity atoms (C_{it}) and total voids (C_t) are 10^{-3} and 10^{-5} , respectively. The binding energy (B_I) of type-I impurity-vacancy complex is taken to be 0.5 eV. The binding energies B_{II} of type-II impurity-vacancy complex are shown in the figure.

C. Formation of Impurity-Vacancy Complexes during Quenching

As discussed in Sec. III C, vacancies make many jumps, and some of them associate with impurity atoms. The formation of impurity-vacancy complexes during

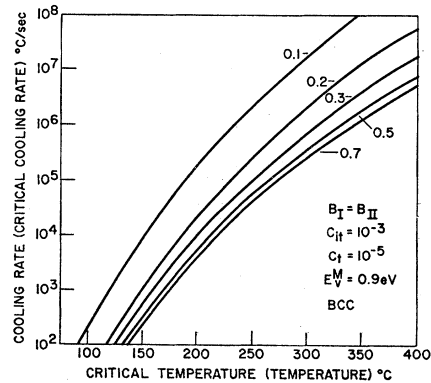


FIG. 21. The values of critical cooling rate versus temperature. The activation energy for the motion of a vacancy is taken to be 0.9 eV. The fractional concentrations of total voids C_t and total impurity atoms C_{it} are taken to be 10^{-5} and 10^{-3} , respectively. The binding energy of type I impurity-vacancy complex is taken to be equal to that of type II. The values of the binding energies are given in the figure. This can be directly used for cooling-rate-versus-critical-temperature relations.

quenching for the interaction up to the next-nearest neighbor can be treated as follows. The kinetic equation is given by Eq. (26):

$$\frac{dC_1}{dt} = -56\nu C_1 C_i \exp\left(-\frac{E_v^M}{kT}\right) + 4\nu C_I \exp\left(-\frac{B_I + E_v^M}{kT}\right) + 4\nu C_{II} \exp\left(-\frac{B_{II} + E_v^M}{kT}\right). \quad (26)$$

It is assumed that no vacancies anneal out during quenching. The total fractional concentration of voids C_t is

$$C_t = \text{const} = C_1 + C_I + C_{II}. \quad (37)$$

Differentiating Eqs. (29), (30), and (37) with respect

to time t , the following equation can be obtained:

$$\frac{dT}{dt} = -\frac{1 + (\xi_I + \xi_{II})(C_i + C_1)}{C_1 C_i (\xi_I' + \xi_{II}')} \frac{dC_1}{dt}, \quad (38)$$

where

$$\xi_I' = -\frac{8B_I}{kT^2} \exp\left(\frac{B_I}{kT}\right), \quad (39)$$

$$\xi_{II}' = -\frac{6B_{II}}{kT^2} \exp\left(\frac{B_{II}}{kT}\right). \quad (40)$$

The rate of the formation of single vacancies at equilibrium is given by the first term of Eq. (26), i.e.,

$$\left(\frac{dC_1}{dt}\right)_e = -56\nu C_1 C_i \exp\left(-\frac{E_v^M}{kT}\right). \quad (41)$$

Equation (38) can be rewritten as

$$\left(\frac{dT}{dt}\right)_{T=T^*} = -\left(\frac{28\nu_1 k T^2 [1 + 2\{4 \exp(B_I/kT) + 3 \exp(B_{II}/kT)\} (C_i + C_1)]}{\{4B_I \exp(B_I/kT) + 3B_{II} \exp(B_{II}/kT)\} \exp(E_v^M/kT)}\right)_{T=T^*}. \quad (42)$$

When the total fractional concentration of voids C_t and the total fractional concentration of impurity atoms are known, Eqs. (35) and (36) can be used. The right-hand side of Eq. (42) is called the critical cooling rate. The values of the critical cooling rate are plotted in Figs. 21 and 22. The values of the total fractional concentration of impurity atoms C_{it} and the total concentration of voids C_t are taken to be 10^{-3} and 10^{-5} , respectively. Figure 21 shows how the critical temperatures change with cooling rate and the binding energy of vacancy impurity. The critical temperature becomes higher as the binding energy does. Figure

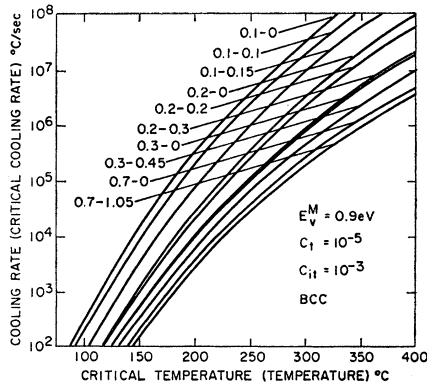


FIG. 22. The values of critical cooling rate versus temperature. The activation energy for the motion of a vacancy is taken to be 0.9 eV. The fractional concentrations of total voids C_t and total impurity atoms C_{it} are taken to be 10^{-5} and 10^{-3} , respectively. The binding energies of type-I and type-II impurity-vacancy complexes are given in the figure, for example, eV. This can be directly used for cooling-rate-versus-critical-temperature relations.

22 shows that the critical temperature becomes higher as B_{II} does, for constant B_I . The values of B_I and B_{II} are shown. The fractional concentrations of free single vacancies and of impurity-vacancy complexes of types I and II after a quench are plotted in Fig. 23 as a function of cooling rate. The total fractional concentrations of impurity and total voids were chosen to be 10^{-3} and 10^{-5} , respectively. The

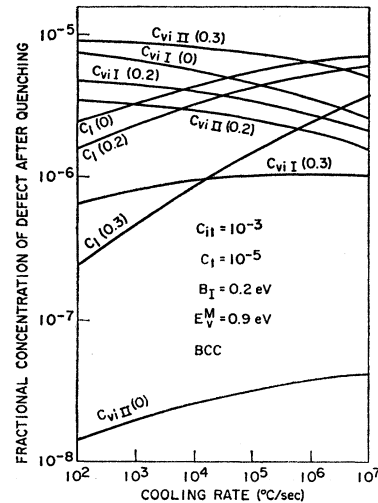


FIG. 23. The fractional concentrations of free vacancies C_1 and type I ($C_{vi I}$) and type II ($C_{vi II}$) impurity-vacancy complexes after quenching versus cooling rate. The fractional concentrations of total voids C_t and total impurity atoms C_{it} are taken to be 10^{-5} and 10^{-3} , respectively. The activation energy for the motion of a vacancy is 0.9 eV. The binding energy of type-I impurity-vacancy complex is taken to be 0.2 eV. The binding energies of type-II impurity-vacancy complexes are given in the figure.

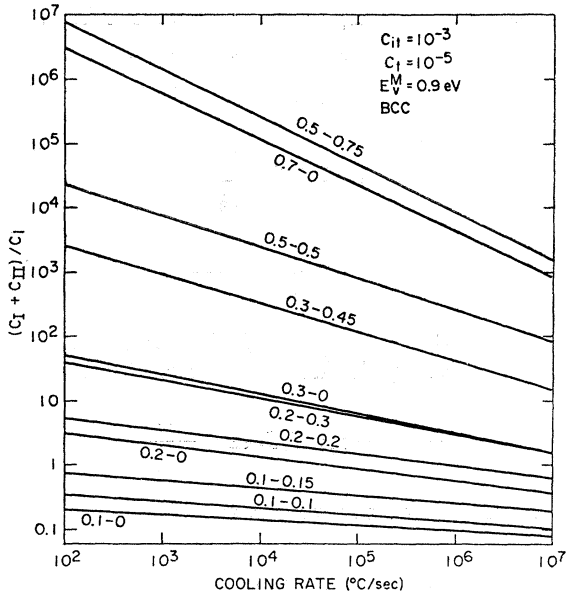


FIG. 24. The logarithm of the ratio of the fractional concentration of impurity-vacancy complexes to that of free vacancies after quenching versus the logarithm of cooling rate. The fractional concentrations of total voids C_I and total impurity atoms C_{II} are taken to be 10^{-5} and 10^{-3} , respectively. The activation energy for the motion of a single vacancy is taken to be 0.9 eV. The binding energies of type-I (B_I) and type-II (B_{II}) impurity-vacancy complexes are shown in the figure. For example, 0.5-0.75 means $B_I=0.5$ and $B_{II}=0.75$ eV.

binding energy of type-I impurity-vacancy complexes was chosen to be 0.2 eV. The binding energies of type-II impurity-vacancy complexes are shown in the figure. The activation energy for the migration of a vacancy is chosen to be 0.9 eV, which case is close to the case of iron. The ratio of the sum of the fractional concentrations of type-I and type-II impurity-vacancy complexes to the fractional concentration of free single

vacancies after quenching is plotted in Fig. 24. Figure 24 shows straight lines corresponding to Fig. 13 for the nearest-neighbor interaction. For $B_{II}=0$ the ratio in Fig. 24 is close to that in Fig. 13. In this figure the total fractional concentration of impurity and total voids were also chosen to be 10^{-3} and 10^{-5} , respectively. The activation energy for the migration of a vacancy is also chosen to be 0.9 eV.

V. SUMMARY

(1) In body-centered cubic crystals the next-nearest-neighbor interaction between an impurity atom and a vacancy is as important as the nearest-neighbor interaction.

(2) Kinetic equations between vacancies and impurity atoms for the nearest-neighbor interaction and for the nearest- and next-nearest-neighbor interaction have been presented.

(3) Applications of these equations to reactions during quenching and aging have been discussed in detail.

(4) The quenched state can be estimated by calculating the critical temperature or freezing temperature. The critical temperatures for the formation of vacancy-impurity atom complexes are near 200°C for the case of iron. The simple analytical treatment gives results which are in good agreement with the actual numerical integration of the kinetic equations by a digital computer.

ACKNOWLEDGMENTS

The author is grateful for the continuous interest and encouragement of O. C. Simpson and J. S. Koehler, and for stimulating discussion with J. S. Koehler. The editorial assistance of R. E. Flink and C. A. Lode is greatly appreciated.